PREPARATION AND ADSORPTION PROPERTIES OF CHITOSAN/SILICA/Fe_3O_4 NANOCOMPOSITE

MOHAMED EL-SAKHAWY,[*] AHMED SALAMA,[*] AHMED K. EL-ZIATY[**] and HAZEM HASSAN[***]

[*]*Cellulose and Paper Department, National Research Centre, 33, El-Bohouth St., Dokki, P.O. 12622, Giza, Egypt*
[**]*Chemistry Department, Faculty of Science, Ain Shams University, Abbassia, Cairo, Egypt*
[***]*Drinking-Water and Sewage Company, Central Labs, Ramses St., Cairo, Egypt*
✉ *Corresponding author: Mohamed El-Sakhawy, elsakhawy@yahoo.com*

Received May 19, 2019

Chitosan-based nanocomposites have been developed to promote the adsorption of water pollutants. In the current work, a chitosan/silica (CS) hybrid was employed as support for the immobilization of iron oxide nanoparticles (Fe_3O_4) to form a chitosan/silica/Fe_3O_4 (CS/Fe_3O_4) nanocomposite. The chitosan, CS and CS/Fe_3O_4 materials were examined by FTIR, XRD, TGA, SEM and TEM analyses. Uniform spherical magnetic nanoparticles of ~20 nm were formed. The effect of the iron oxide formation on the adsorption capacity and COD reduction of methylene blue (MB) was calculated. The best interpretation for the equilibrium data was given by the Langmuir isotherm, and the maximum adsorption capacity reached 285 mg/g. The CS/Fe_3O_4 nanocomposite displayed higher adsorption capacity in a slightly basic medium. This article proposes the CS/Fe_3O_4 nanocomposite as a new adsorbent for the removal of organic dyes from wastewater.

Keywords: chitosan, silica, iron oxide, hybrid, water purification

INTRODUCTION

Water pollutants, especially organic compounds, are continuously produced as waste from various industries, such as textiles, ceramics, paper and printing.[1,2] Among them, organic dyes are visible due to their brightness and most of them infect groundwater, causing problems to human health and marine life.[3,4] Different physical, chemical and biological techniques are applied for the treatment of aqueous solutions polluted with organic dyes.[5,6] Most of these techniques are expensive and time-consuming, therefore they are rarely used.

Recently, adsorption has emerged as a low-cost and fast strategy for the removal of inorganic and organic substances from the aqueous environment.[7,8] Coupling of polysaccharides and magnetite produces new materials, with high adsorption properties, used also as heterogeneous catalysts, to treat wastewater.[9] However, magnetite nanoparticles agglomerate easily, which will reduce their adsorption capacity. The preparation of polysaccharide/Fe_3O_4 nanocomposite can reduce the agglomeration properties of the formed nanoparticles and promote their adsorption performance. For example, bacterial cellulose/magnetite nanocomposites were investigated for the adsorption of chromium (VI). Magnetic nanoparticles have uniform dispersion in the bacterial cellulose matrix.[10] Salama *et al*. prepared carboxymethyl cellulose/Fe_3O_4 nanocomposite by co-precipitation of iron (II) and (III) salts. The nanocomposite, having uniform spherical magnetic nanoparticles with a diameter of ~25 nm, was applied as an efficient adsorbent for MB removal from wastewater.[11] Also, a Fe_3O_4 core coated with different amounts of soluble bio-based materials was developed for the removal of Crystal Violet cationic azo dye.[9] A chitosan/iron oxide nanocomposite was prepared as an eco-friendly bio-adsorbent for MB-polluted water remediation.[12] Removing cadmium from

wastewater using iron oxide nanoparticles was also investigated.[13] Also, stable Fe_3O_4/cellulose nanocomposites were prepared through the co-precipitation method. These nanocomposites could enhance the catalytic activity for the degradation of MB.[14]

Polysaccharides have recently emerged as sustainable and biocompatible materials for a variety of applications.[15,16] Chitosan has been examined as adsorbent due to the presence of amino and hydroxyl groups, which can serve as active sites for adsorption.[17] Moreover, silica gel precursors exhibit quick *in-situ* silica network formation in the presence of ethanol and water *via* the sol-gel technique, forming glassy, homogeneous and transparent materials. Chitosan/silica hybrid materials combine the advantage of the individual components: they are porous and rigid like silica gel and have different functional groups due to chitosan.[18,19] The surface areas and particle size of the nanocomposite control its adsorption capacity. As a result, there is a need to synthesize new absorbents with proper particle sizes. Various nanocomposites based on Fe_3O_4 have been evaluated for industrial and biomedical applications.[20,21]

In this work, the CS/Fe_3O_4 nanocomposite was employed for MB removal from wastewater. This nanocomposite was chosen as a new adsorbent by considering the main advantages: (1) this composite can be produced using the co-precipitation method, (2) its adsorption capacity is high by considering its large surface area and highly active surface sites, (3) the uptake process occurs *via* external adsorption, resulting in very short adsorption and desorption time, (4) the separation of the adsorbent from treated water can be achieved by using an external magnetic field. The following factors were investigated to find the optimum conditions for enhancing treatment efficiency: solution pH, contact time and initial concentration. The current study also measured the capability of the nanocomposite in simultaneously reducing the chemical oxygen demand (COD).

EXPERIMENTAL

Materials

Low viscous chitosan from shrimp shells and tetraethyl orthosilicate (TEOS) (99.9%) were purchased from Sigma Aldrich. The other chemicals, such as ferrous sulfate and ferric chloride, methylene blue and ammonium hydroxide, were of analytical grade and used as received.

CS/Fe_3O_4 nanocomposite preparation

Firstly, chitosan/silica (CS) was prepared as reported in our previous work.[8] In a glass vial, 6 mL of chitosan solution was stirred with ethanol, distilled water, HCl and 2 mL of TEOS. Then, the pH was turned to slightly alkaline by adding ammonia, and the reaction mixture was left until complete gelation. The formed gel was washed with distilled water until neutral pH. The formed gel was divided into two parts. The first part was immersed in 5.2 g of ferric chloride dissolved in 12.5 mL of deoxygenated distilled water. The second part was dissolved in 2.7 g of ferrous sulphate dissolved in 12.5 mL water. The two parts were mixed and deoxygenated again for 20 minutes. The ammonium solution (1.5 M) was then added until the solution became completely black, indicating the formation of magnetite. The resultant black residue was washed several times, dried and sieved to separate the nanocomposite.

Adsorption study

The adsorption studies were performed using the batch method technique. In brief, 0.05 g of dried CS/Fe_3O_4 nanocomposite was soaked in 50 mL of dye solutions with 100 mg/L concentration. After ending the adsorption process under the desired conditions, the solution was separated from the adsorbents by centrifugation for 60 minutes and the dye concentration was calculated using a UNICO UV-2000 spectrophotometer at a wavelength of 664 nm.

Determination of COD reduction in wastewater

The COD was calculated using the dichromate reflux method, as discussed in our previous study.[8] The experiments were carried out in the batch mode at ambient temperature (25 °C). Each flask was filled with a known volume of dye solution, having the desired pH, along with the known weight of nanocomposite. The solutions were withdrawn from the shaker at predetermined time intervals for COD measurements. For investigating the effect of pH on the treatment process, 0.05 g of the adsorbent was mixed with 100 mL of the contaminated sample for 60 minutes, and the treatment was continued in the shaker flask. The same conditions were used to study the effect of time, varying the time intervals.

Characterization

Fourier transform infrared spectroscopy (FT-IR) was performed on an FTIR (Mattson 5000 FTIR spectrometer) in the range of 4000-500 cm^{-1}. Scanning electron microscopy (SEM) was done on a Quanta 250 FEG (Field Emission Gun) attached to an EDX Unit (Energy Dispersive X-ray Analyses), with accelerating voltage of 30 K. Transmission electron microscopy (TEM) images were taken with a JEOL JEM-2100 electron microscope, at 100k× magnification, with an acceleration voltage of 120 kV. An X-ray

diffractometer equipped with an automatic divergent slit Philips diffractometer (type PW 3710) was used. The patterns were obtained with Ni-filtered copper radiation (λ = 1.5404 Å) at 30 kV and 10 mA, with a scanning speed of 2θ = 2.5°/min. Thermogravimetric thermal analyses (TGA) were carried out using Shimadzu-50 thermal analyzer units under N_2 flowing at a rate of 30 mL/min.

RESULTS AND DISCUSSION

Preparation of CS/Fe_3O_4 nanocomposite

Scheme 1 shows the mechanism of CS/Fe_3O_4 nanocomposite formation, which involves the following steps, as shown in Scheme 1. The formation of the silica network proceeds by the sol-gel technique. The triethoxy groups of TEOS hydrolyzed to form silanol groups, which condense subsequently *via* a sol-gel process to form chitosan embedded in the silica hybrid network. The H-bonding between the hydroxyl groups of chitosan and the uncondensed hydroxyl groups of silica increases the homogeneity of the formed hybrid. The CS/Fe_3O_4 nanocomposite was prepared by the co-precipitation method and the magnetic nanoparticles are expected to be embedded and on the surface of the CS hybrid.

Characterization of CS/Fe_3O_4 nanocomposite

The functional groups present in the chitosan, CS and CS/Fe_3O_4 nanocomposite were investigated by FT-IR spectroscopy. Figure 1A displays the chitosan characteristic peaks reported in previous work.[22] A new intense band in the CS hybrid was found between 1090 and 1030 cm^{-1}, and can be associated with the Si– O– Si and Si – O – C vibrations. Moreover, a new peak at 538 cm^{-1} was assigned to the stretching vibration of Fe_3O_4 in the CS/Fe_3O_4 nanocomposite.[23]

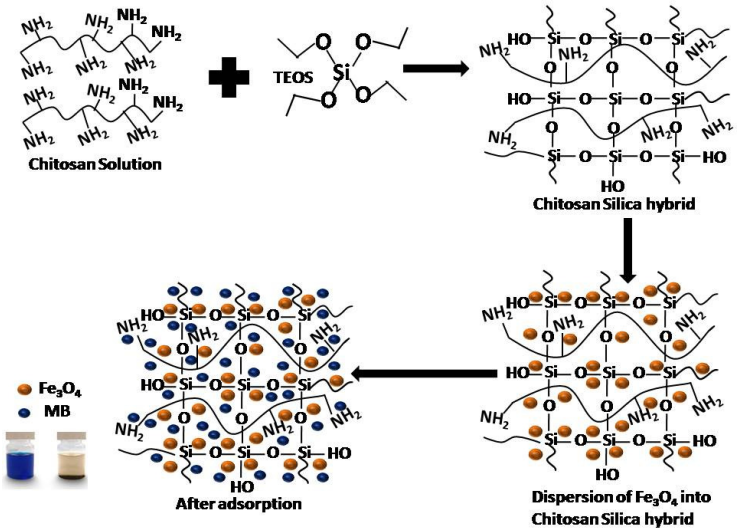

Scheme 1: CS/Fe_3O_4 nanocomposite preparation route

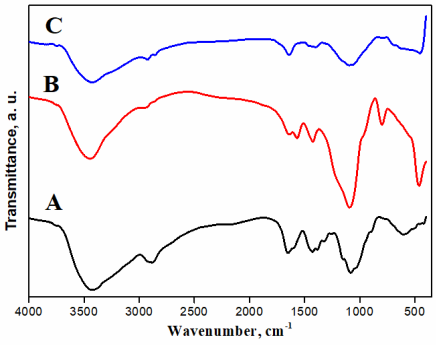

Figure 1: FT-IR spectra of chitosan (A), chitosan/silica hybrid (B) and chitosan/silica/Fe3O4 nanocomposite (C)

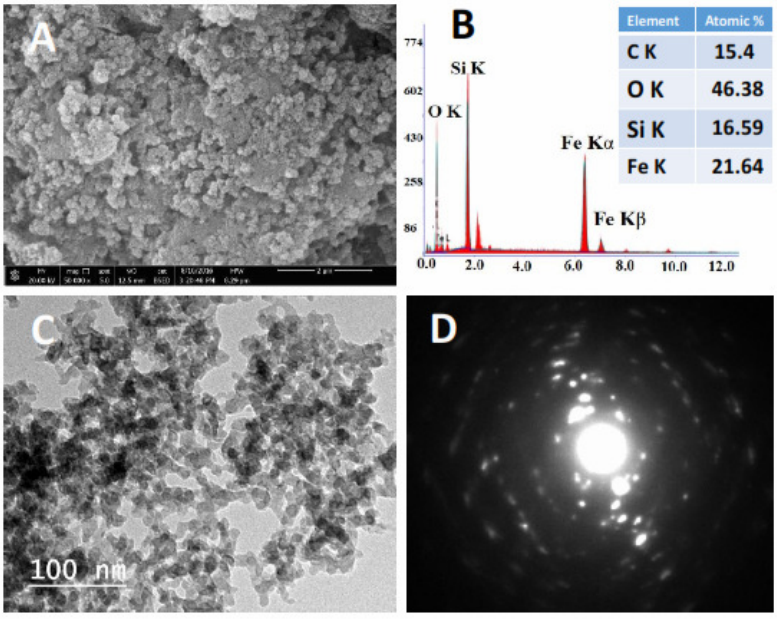

Figure 2: SEM (A), EDX (B), TEM (C) and SAED (D) of CS/Fe_3O_4 nanocomposite

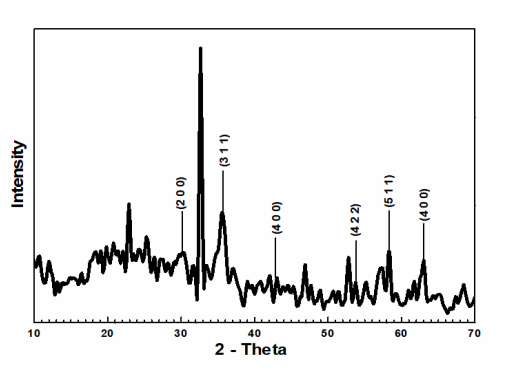

Figure 3: XRD pattern of CS/Fe_3O_4 nanocomposite

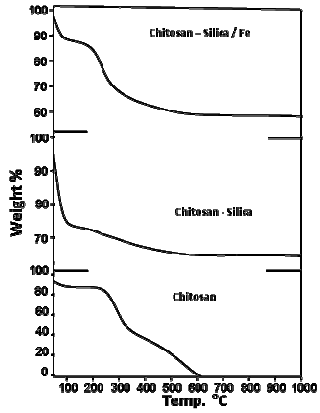

Figure 4: TGA curves of chitosan, CS and CS/Fe_3O_4 nanocomposite

The surface morphology of the CS/Fe_3O_4 nanocomposite was examined using SEM analysis (Fig. 2A). The prepared nanocomposite shows the presence of nanoparticles with ~50 nm length. Moreover, the iron oxide nanoparticles appear to be uniform, which may suggest the role of CS in decreasing the attractive forces among nanoparticles, reducing their aggregation tendency. The EDX results display the atomic% of Si and Fe as 16.6 and 21.6%, respectively, as shown in Figure 2B. The internal structure observed by TEM in Figure 2C exhibits homogeneous and densely packed nanospheres, with a mean diameter of ~20 nm. The selected area electron diffraction showed a high degree of crystallinity for the formed Fe_3O_4 nanoparticles (Fig. 2D).

The XRD pattern of the CS/Fe_3O_4 nanocomposite is shown in Figure 3. The nanocomposite exhibits peaks at 2θ values of 30°, 35.6°, 43°, 54.5°, 58° and 63°, corresponding to the typical Miller indices of an inverse spinel magnetite: (2 0 0), (3 1 1), (4 0 0), (4 2 2), (5 1 1) and (4 0 0), respectively. The pattern was found to coincide with that from the JCPDS database for magnetite (JCPDS file 19629; Joint Committee on Powder Diffraction: Swarthmore, PA). XRD suggests the successful formation of crystalline iron oxide on the CS hybrid.

The thermal behavior curves of chitosan, CS and CS/Fe_3O_4 nanocomposite are shown in Figure 4. Generally, all the hybrid samples undergo two stages of degradation: (i) loss of moisture and (ii) decomposition of chitosan chains. Chitosan exhibits weight loss in two stages. The first weight loss (7%) occurred at 50-155 °C, arising from the dehydration of chitosan. The second step of weight loss (93%) at 211-630 °C is due to the decomposition of chitosan chains. Moreover, CS shows two stages of decomposition: at 90 °C, with an estimated mass loss of 25%, and a weight loss of 33% in the temperature range of 165-630 °C is due to the decomposition of the polymeric network. This signifies that the formation of the CS hybrid involves crosslinking and the results exhibit obviously lower weight loss compared to that of neat chitosan, due to the presence of stable silica (about 42% residue). However, CS/Fe_3O_4 showed a mass loss of 7.5% at 55-127 °C and the second step occurs within the temperature range of 146-442 °C, with an estimated mass loss of 34%, leaving 66% iron oxide and silica residues.

MB adsorption properties of CS/Fe_3O_4 nanocomposite

The performance of CS and CS/Fe_3O_4 nanocomposite in MB removal from aqueous solutions was explored. The effect of various parameters, including solution pH, contact time and initial MB concentration, on the adsorption performance was assessed.

The of MB dye onto the chitosan/silica/magnetite nanocomposite adsorbents was pH-dependence and the MB adsorption capacity increasing at a higher pH. The solution pH controls the ionization level of the dye and the nanocomposite in the solution, thereby promoting the surface charge.[18] The effect of pH on the adsorption performance of CS and CS/Fe_3O_4 nanocomposite was calculated as displayed in Figure 5 (1). For both samples, the adsorption rate gradually increased to reach the optimum adsorption at pH 7 and reached 62 and 70 mg/g for CS and the CS/Fe_3O_4 nanocomposite, respectively. Under the same experimental conditions, the adsorption capacity was significantly higher for the CS/Fe_3O_4 nanocomposite, compared with that of the CS hybrid. Higher solution pH values decreased the concentration of H^+ ions, which eventually increased the accessible binding sites for MB adsorption. The pH results suggested that the adsorption of MB onto the CS/Fe_3O_4 nanocomposite followed the ionic interaction mechanism. The MB dye adsorption capacity of the nanocomposite being pH-dependent, it increased at a higher pH. In fact, considering that the pKa of MB is 3.8, for higher pH values, the cationic species were the preponderant MB species in the solutions.

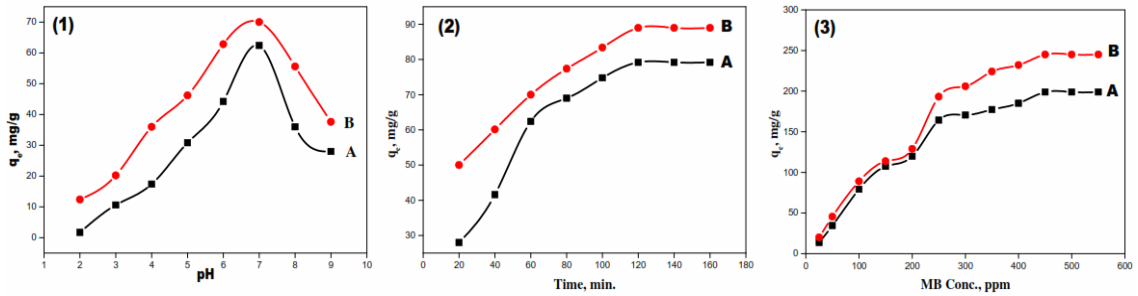

Figure 5: (1) Effect of pH on MB adsorption onto CS (A) and CS/Fe_3O_4 (B) (MB: 100 mg/L, sample dose: 0.05 g/50 mL and contact time: 60 min); (2) Effect of time on MB adsorption onto CS (A) and CS/Fe_3O_4 (B) (MB: 100 mg/L, sample dose: 0.05 g/50 mL and pH: 7.0); (3) Effect of MB concentration on MB adsorption onto CS (A) and CS/Fe_3O_4 (B) (sample: 0.05 g/50 mL, pH: 7 and contact time 24 h)

The rate of MB uptake also depends on the contact time between the binding sites of the adsorbent and the adsorbate molecules.[24] The surface structure of the CS and CS/Fe_3O_4 nanocomposite plays an important role in the adsorption process. The adsorption of MB onto the CS and the CS/Fe_3O_4 nanocomposite was found to be rapid during the first 120 minutes, after which it slowed down and the curve flattened off as the contact time increased (~120

to ~160 min). It finally reached a plateau after 160 min for both CS and CS/Fe_3O_4, as shown in Figure 5 (2).

The high number of vacant adsorption sites starts to decrease and the adsorption sites become more difficultly accessible with increasing time. Figure 5 (3) shows that, as the MB initial concentration increased, the adsorption rate was markedly increased until an MB concentration of 250 mg/L, after which the adsorption rate increased slowly till 198 and 245 mg/g at an MB concentration of 550 ppm for CS and the CS/Fe_3O_4 nanocomposite, respectively, due to the occupation of adsorption sites. The adsorption capacity tends to level off with higher concentrations beyond 550 ppm due to the saturation of the active sites.

Reusability of nanocomposite for MB adsorption

The desorption and reusability of an adsorbent are crucial parameters to evaluate its suitability for application. The behavior of the chitosan/silica/magnetite nanocomposite was examined during four adsorption–desorption cycles and the results are displayed in Figure 6. In 0.1 M HCl solution, the adsorption capacity decreased slightly from 97%, in the first cycle, to 93%, after the fourth cycle. To conclude, the chitosan/silica/magnetite nanocomposite can be applied repeatedly as an efficient adsorbent for cationic dyes removal.

Adsorption kinetics

The pseudo-first order and pseudo-second-order models were applied to simulate and understand the adsorption kinetics of MB onto CS and CS/Fe_3O_4 nanocomposite. The pseudo-first order model assumes that the rate-limiting step is a physical process. The pseudo-second order model assumes chemical adsorption through the sharing or exchange of electrons. Pseudo-first and pseudo-second models are expressed as Equations (1) and (2), respectively:[25]

$$\log (q_e - q_t) = \log (q_e) - \frac{K1}{2.303} t \quad (1)$$

$$\frac{t}{qt} = \frac{t}{qe} + \frac{1}{k2qe2} \quad (2)$$

The rate constants (k_1 and k_2), the correlation coefficients and the calculated $q_{e,cal}$ for the two models are displayed in Table 1. The calculated results showed that the adsorption followed the pseudo-second order model. This result suggests chemical interaction between the MB and the nanocomposite surfaces during the adsorption process.

The Langmuir and Freundlich models were applied to determine the isotherm parameters. The Langmuir isotherm assumes monolayer adsorption on a homogeneous surface. This isotherm equation can be written in a linearized form as follows:[26]

$$\frac{C_e}{q_e} = \frac{K_s}{q_{\max}} + \frac{C_e}{q_{\max}} \quad (3)$$

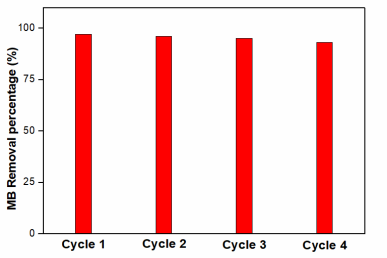

Figure 6: Reusability of chitosan/silica/magnetite nanocomposite for MB adsorption

Table 1
Kinetic parameters for MB adsorption onto CS/Fe_3O_4 nanocomposite

Pseudo-first order model				Pseudo-second order model		
$q_{e,exp}$ (mg/g)	$q_{e,cal}$ (mg/g)	K_1(min^{-1})	R^2	$q_{e,cal}$ (mg/g)	K_2 g(mg min)$^{-1}$	R^2
89	63	0.023	0.960	100	3.9 x 10^{-4}	0.994

Table 2
Parameters for MB adsorption onto CS/Fe_3O_4 according to different equilibrium models

Langmuir isotherm constants			Freundlich isotherm constants		
K_s (mg/L)	q_m (mg/g)	R^2	P (mg/g)	n	R^2
42.7	285	0.963	18.19	2.024	0.840

Table 3
Maximum MB adsorption capacities of composite materials

Adsorbent	Maximum MB adsorption (mg/g)	References
Chitosan coated magnetic mesoporous silica nanoparticles	43.03	[1]
Chitosa/silica/ZnO nanocomposite	293.3	[8]
Chitosa/FeO nanocomposite	5.12	[12]
Chitosan-coated quartz	45.5	[19]
Chitosan/silica/magnetite nanocomposite	285	This work

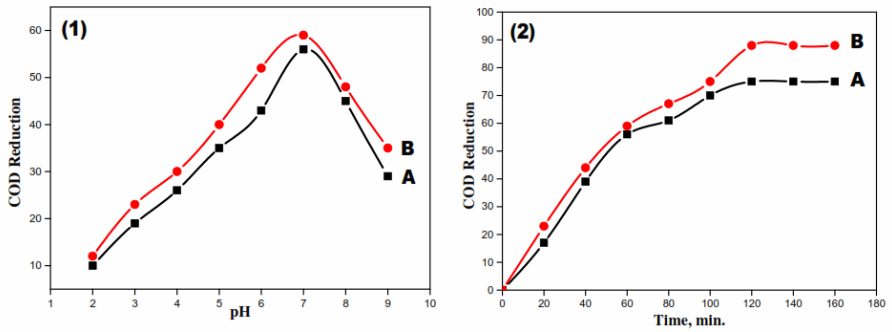

Figure 7: (1) Effect of pH on COD of CS (A) and CS/Fe_3O_4 nanocomposite (B); (2) Effect of contact time on COD of chitosan/silica (A) and chitosan/silica/Fe_3O_4 (B)

The plot of C_e/q_e against C_e for the experimental data displayed a high correlation coefficient ($R^2 > 0.96$). Table 2 indicates that the Langmuir model can describe the adsorption of MB onto the CS Fe_3O_4 nanocomposite. From the slope and the intercept of the straight line, the values of q_{max} and K_s are estimated to be 107.5 mg/g and 18.33 mg/L, respectively. The Langmuir model assumes monolayer adsorption of MB onto CS/Fe_3O_4 and that all sites have equal energies and enthalpies.

The Freundlich equation is given by:

$$\log q_e = \frac{1}{n}\log C_e + \log P \quad (4)$$

The Freundlich parameters display a linear coefficient of 0.921. Moreover, the values of the Freundlich model constants P and n are 15 and 2.59, respectively. These results show that this model does not describe MB adsorption onto CS/Fe_3O_4.

Table 3 compares the adsorption capacity of this material with that of other similar materials. Considering these data, it could be concluded that the prepared material is a competitive adsorbent for MB.

COD studies

The remaining COD concentration was measured after treating the solutions with CS and CS/Fe_3O_4 nanocomposite. The influence of pH on the COD value was examined, starting with 1086 mg/L, which is the blank COD concentration. Figure 7 (1) determines the percent reduction in COD for various pH values. The results showed that COD reduction recorded maximum values of 56% and 59% at pH 7 for CS and the CS/Fe_3O_4 nanocomposite, respectively.

The effect of contact time on COD was examined at pH 7, while the contact time ranged from 0 to 160 minutes. Figure 7 (2) indicates that increasing the contact time up to 120 minutes enhances the COD reduction values. The maximum result was recorded at 120 minutes. It was found that the maximum COD values were

measured as 75 and 88 for CS and the CS/Fe_3O_4 nanocomposite, respectively.

CONCLUSION

A CS hybrid was used to develop a CS/Fe_3O_4 nanocomposite to be applied for remediation of dye-polluted water. The study compared the adsorption capacity of CS and CS/Fe_3O_4 nanocomposite to evaluate the influence of Fe_3O_4 nanoparticles on the adsorption capacity. The results showed that the presence of iron oxide nanoparticles enhances the adsorption capacity. MB adsorption was studied from aqueous solutions, and the adsorption was found to be most effective at pH 7. The adsorption followed the Langmuir isotherm and was observed to be a feasible process. The developed material exhibited a high removal capacity and COD reduction, therefore this novel material performs as a promising candidate for application in dye-polluted wastewater treatment.

REFERENCES

[1] Y. Li, Y. Zhou, W. Nie, L. Song and P. Chen, *J. Porous Mater.*, **22**, 1383 (2015), https://doi.org/10.1007/s10934-015-0017-7

[2] L. Wang, J. Zhang and A. Wang, *Desalination*, **266**, 33 (2011), https://doi.org/10.1016/j.desal.2010.07.065

[3] R. Fabryanty, C. Valencia, F. E. Soetaredjo, J. N. Putro, S. P. Santoso *et al.*, *J. Environ. Chem. Eng.*, **5**, 5677 (2017), https://doi.org/10.1016/j.jece.2017.10.057

[4] S. Sharma and A. Bhattacharya, *Appl. Water Sci.*, **7**, 1043 (2017), https://doi.org/10.1007/s13201-016-0455-7

[5] A. Salama, N. Shukry and M. El-Sakhawy, *Int. J. Biol. Macromol.*, **73**, 72 (2015), http://dx.doi.org/10.1016/j.ijbiomac.2014.11.002

[6] X. An, D. Cheng, L. Dai, B. Wang, H. J. Ocampo *et al.*, *Appl. Catal. B Environ.*, **206**, 53 (2017), https://doi.org/10.1016/j.apcatb.2017.01.021

7 M. Monier, D. M. Ayad, Y. Wei and A. A. Sarhan, *J. Hazard. Mater.*, **177**, 962 (2010), https://doi.org/10.1016/j.jhazmat.2010.01.012

[8] H. Hassan, A. Salama, A. K. El-Ziaty and M. El-Sakhawy, *Int. J. Biol. Macromol.*, **131**, 520 (2019), https://doi.org/10.1016/j.ijbiomac.2019.03.087

[9] G. Magnacca, A. Allera, E. Montoneri, L. Celi, D. E. Benito *et al.*, *ACS Sustain. Chem. Eng.*, **2**, 1518 (2014), https://doi.org/10.1021/sc500213j

[10] A. Stoica-Guzun, M. Stroescu, S. I. Jinga, N. Mihalache, A. Botez *et al.*, *Int. J. Biol. Macromol.*, **91**, 1062 (2016), https://doi.org/10.1016/j.ijbiomac.2016.06.070

[11] A. Salama, S. Etri, S. A. A. Mohamed and M. El-Sakhawy, *Carbohyd. Polym.*, **189**, 138 (2018), https://doi.org/10.1016/j.carbpol.2018.02.016

[12] M. Keshvardoostchokami, F. Piri and A. Zamani, *Micro Nano Lett.*, **12**, 338 (2017), https://doi.org/10.1049/mnl.2016.0681

[13] M. H. Ehrampoush, M. Miria, M. H. Salmani and A. H. Mahvi, *J. Environ. Heal. Sci. Eng.*, **13**, 1 (2015), https://doi.org/10.1186/s40201-015-0237-4

[14] Q. Lu, Y. Zhang, H. Hu, W. Wang, Z. Huang *et al.*, *Nanomaterials*, **9**, 275 (2019), https://doi.org/10.3390/nano9020275

[15] M. El-Sakhawy, A. Salama, S. Kamel and H. S. Tohamy, *Cellulose Chem. Technol.*, **53**, 667 (2019), https://doi.org/10.35812/CelluloseChemTechnol.2019.53.65

[16] M. El-Sakhawy, S. Kamel, A. Salama and H. S. Tohamy, *Cellulose Chem. Technol.*, **52**, 193 (2018), http://www.cellulosechemtechnol.ro/pdf/CCT3-4(2018)/p.193-200.pdf

[17] W. S. Wan Ngah, L. C. Teong and M. A. K. M. Hanafiah, *Carbohyd. Polym.*, **83**, 1446 (2011), https://doi.org/10.1016/j.carbpol.2010.11.004

[18] A. Salama and P. Hesemann, *Int. J. Biol. Macromol.*, **111**, 762 (2018), https://doi.org/10.1016/j.ijbiomac.2018.01.049

[19] B. Zhao, X. Zhang, C. Dou and R. Han, *Desalin. Water Treat.*, **55**, 1598 (2015), https://doi.org/10.1080/19443994.2014.925834

[20] H. S. Hassan, M. F. Elkady, A. A. Farghali, A. M. Salem and A. I. A. El-Hamid, *J. Taiwan Inst. Chem. Eng.*, **78**, 307 (2017), https://doi.org/10.1016/j.jtice.2017.06.021

[21] Y. Jiao, C. Wan, W. Bao, H. Gao, D. Liang *et al.*, *Carbohyd. Polym.*, **189**, 371 (2018), https://doi.org/10.1016/j.carbpol.2018.02.028

[22] A. Salama, *Cellulose Chem. Technol.*, **52**, 903 (2018), http://www.cellulosechemtechnol.ro/pdf/CCT9-10(2018)/p.903-907.pdf

[23] I. V. Pylypchuk, D. Kołodyńska, M. Kozioł and P. P. Gorbyk, *Nanoscale Res. Lett.*, **11**, 168 (2016), https://doi.org/10.1186/s11671-016-1363-3

[24] J. Ma, F. Yu, L. Zhou, L. Jin, M. Yang *et al.*, *ACS Appl. Mater. Interfaces*, **4**, 5749 (2012), https://doi.org/10.1021/am301053m

[25] A. Salama, *Nanotechnol. Monit. Manag.*, **6**, 159 (2016), https://doi.org/10.1016/j.enmm.2016.10.003

[26] R. Zhao, Y. Wang, X. Li, B. Sun and C. Wang, *ACS Appl. Mater. Interfaces*, **7**, 26649 (2015), https://doi.org/10.1021/acsami.5b08403